Soft Matter

PAPER

View Article Online
View Journal | View Issue

Cite this: *Soft Matter*, 2014, **10**, 8737

Universality of the network-dynamics of the cell nucleus at high frequencies

Omar F. Zouani,*[ab] Thomas Dehoux,*[cd] Marie-Christine Durrieu[ab] and Bertrand Audoin[cd]

Received 29th April 2014
Accepted 2nd September 2014

DOI: 10.1039/c4sm00933a

www.rsc.org/softmatter

The interior of the cell nucleus is comparable to a solid network bathed in an interstitial fluid. From the extrapolation of low frequency data, it is expected that such network should dictate the response of the nucleus to mechanical stress at high frequencies, described by unique elastic moduli. However, none of the existing techniques that can probe the mechanical properties of cells can exceed the kHz range, and the mechanics of the nuclear network remain poorly understood. We use laser-generated acoustic waves to probe remotely the stiffness and viscosity of nuclei in single cells in the previously unexplored GHz range with a ~100 nm axial resolution. The probing of cells at contrasted differentiation stages, ranging from stem cells to mature cells originating from different tissues, demonstrates that the mechanical properties of the nuclear network are common across various cell types. This points to an asymptotically increasing influence of a solid meshwork of connected chromatin fibers.

1 Introduction

Nuclear mechanics and structural integrity have been shown to be critical for a variety of cellular functions, and their alteration is correlated to many diseased conditions, such as cancer or muscular dystrophy.[1–3] It has also been postulated that the access of specific transcription factors to their binding sites and gene expression can be modulated by nuclear deformations.[4,5] Understanding nuclear mechanics is thus essential for the analysis of the mechanisms underlying fundamental biological processes.

The interior of the nucleus has a complex composition that consists mainly of DNA molecules packaged by proteins to form chromatin fibers, and also contains other subcompartments. This sophisticated structure yields an intricate mechanical behavior resembling that found in polymer networks.[6] The infinite number of conformations of the nuclear components at various length scales yields a multiplicity of closely-spaced relaxation times, and leads to a weak power-law rheology of the nucleus.[7] This behavior can be understood by analogy with a meshwork of chromatin fibers bathed in a cytosol-like fluid.[8]

Although the composition of the cytoplasm differs from that of the nucleus, the cytoplasm too has been compared to an elastic solid meshwork surrounded by an interstitial fluid.[9] Interestingly, microrheological measurements, in which one tracks the Brownian motion of microparticles embedded in the cell subcompartments, have revealed that the frequency-dependence of the mechanical properties of the cytoplasm is very similar to that of the nucleus.[6] The rotation of magnetic beads attached to the outer surface of the cell by binding to the cytoskeleton, namely magnetic bead cytometry, has revealed the same weak power-law rheology up to 100 kHz.[10] There is thus a clear analogy between the nucleus and the cytoplasm from a rheological point of view.

At high frequencies, the cytoplasmic network is expected to dominate the mechanical response.[11] Building on the extrapolation far outside the kHz measurement range of magnetic bead cytometry,[10] a unique elastic modulus has been hypothesized to exist in the cytoplasmic region at GHz frequencies. This behavior, averaged over the whole cell structure, was thus attributed to a purely elastic behavior of the cytoskeletal network alone. Since the nucleus is in general more dense than the cytoplasm, we also expect a universal behavior of the nucleus. However, none of the existing techniques that can probe the mechanical properties of cells can exceed the kHz range, and the universality of the network dynamics has therefore not yet been measured.

Inelastic light scattering by acoustic waves, namely Brillouin light scattering (BLS), produces frequency shifts in the GHz range, and allows spectroscopic probing of elastic properties in the glassy state of amorphous solids, colloids or suspensions. Recent implementation of confocal Brillouin microscopy has allowed imaging crystalline lens in a mouse eye with a 60 μm axial resolution,[12] limited by the weakness of the scattered signal. The cells thickness is however a few micrometers,[13] and can even be less for cells with large peripheral regions,[14] such as

[a]*Univ. Bordeaux, Institut Européen de Chimie et Biologie, CNRS UMR 5248, F-33607 Pessac, France. E-mail: omar.zouani@avegem.com*

[b]*Univ. Bordeaux, Bioingénierie Tissulaire, INSERM U1026, F-33076 Bordeaux, France*

[c]*Univ. Bordeaux, I2M, UMR 5295, F-33405 Talence, France. E-mail: t.dehoux@i2m.u-bordeaux1.fr*

[d]*CNRS, I2M, UMR 5295, F-33405 Talence, France*

adhering or migrating cells. Single cell inspection therefore requires observation of light scattering from an extremely small volume not compatible with state-of-the-art BLS.

To bypass this limitation, here we use the controlled emission of GHz acoustic waves to enhance the scattering. This technique called picosecond ultrasonics (PU), developed 30 years ago,[15,16] allows observing light scattering with a broad frequency range extending up to 1 THz, a sub-micrometer lateral resolution and a nanometer in-depth resolution. Contrary to methods relying on contact probes such as atomic force microscopy[17] or micropipette aspiration,[7] PU is an all-optical technique that probes remotely the mechanical properties of the material. Lately, PU has allowed measuring non-invasively the dynamics of the cellulose fiber network within plant cell walls[18] as well as the inner mechanical properties of single-cell nuclei at GHz frequencies.[19]

In this article, we used PU to investigate the GHz dynamics of single-cell nuclei. We probed cells at various differentiation stages, ranging from stem cells to mature cells originating from vastly different tissues, as well as cancerous cells. We thereby demonstrate the existence of a unique nuclear stiffness at GHz frequencies, which we attribute to the contribution of the solid network of chromatin fibers.

2 Results

2.1 GHz dynamics of single cell nuclei

We cultured cells on a metal plate for photoelastic transduction (see details in Material and methods for cell culture and reagents). Fig. 1(a) shows a typical white-light image of an osteoblast cell on titanium. The low-energy coaxial laser pump and probe beams are focused through the top of the nuclear region at the metal–cell interface [see Fig. 1(b)]. The femtosecond pump pulses are initially absorbed in the metal plate over a nanometer depth. The ensuing ultrafast thermal dilatation of the metal launches a compressional sound pulse. Due to metal–cell contact, the compressional sound pulse is simultaneously transmitted to the cell, and propagates through the nucleus. This pulse induces infinitesimal strain with an amplitude of $\sim 10^{-6}$. The typical acoustic frequency bandwidth extends up to 150 GHz. The transient optical reflectivity change δR induced by acoustic propagation is measured *via* optical probe pulses. The photoelastic interaction of the probe light of wavelength $\lambda = 400$ nm with the acoustic pulse propagating in the transparent nucleus [see inset of Fig. 1(b)] produces so-called Brillouin oscillations[15] at a frequency $f = 2n_r V/\lambda$, where n_r and V are the refractive index and the longitudinal sound velocity in the nucleus, respectively.

Fig. 2(a) shows typical δR transients measured (plain lines) in osteosarcoma cells. The experiments were performed on the intranuclear region because it occupies the entire cell thickness, as shown by the confocal microscopy images in Fig. 3(a) and (b). The transient δR obtained in the intranuclear region of the osteosarcoma cells [Fig. 2(a)] features a damped Brillouin oscillation of the form $\delta R(t) \propto \sin(2\pi ft)\exp(-\alpha t)$. The frequency f and lifetime $1/\alpha$ of this oscillation are related to sound velocity and attenuation, respectively. For osteosarcoma cells of this relatively large thickness (>1 μm), we obtained values of $f = 25.7 \pm 0.6$ GHz and $\alpha = 7 \pm 3$ ns^{-1} from a Fourier transform [Fig. 2(b)].

The transient δR obtained in the intranuclear region of thin osteoblast cells [Fig. 2(c)] features the same Brillouin oscillation, in addition to a lower-frequency step-like reflectivity variation due to acoustic-induced motion of the free surface of the cell. To illustrate the physics of signal formation in thin cells, we modelled the photoelastic interaction, as detailed in the Material and methods section. The calculation, plotted with dashed lines in Fig. 2(c), was fitted to the data by adjusting

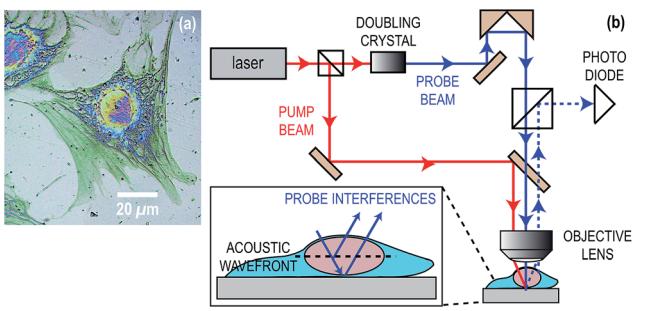

Fig. 1 (a) White-light top-view of a typical osteoblast cell on titanium. (b) Simplified setup. Inset: photoelastic interaction. Bar: 20 μm.

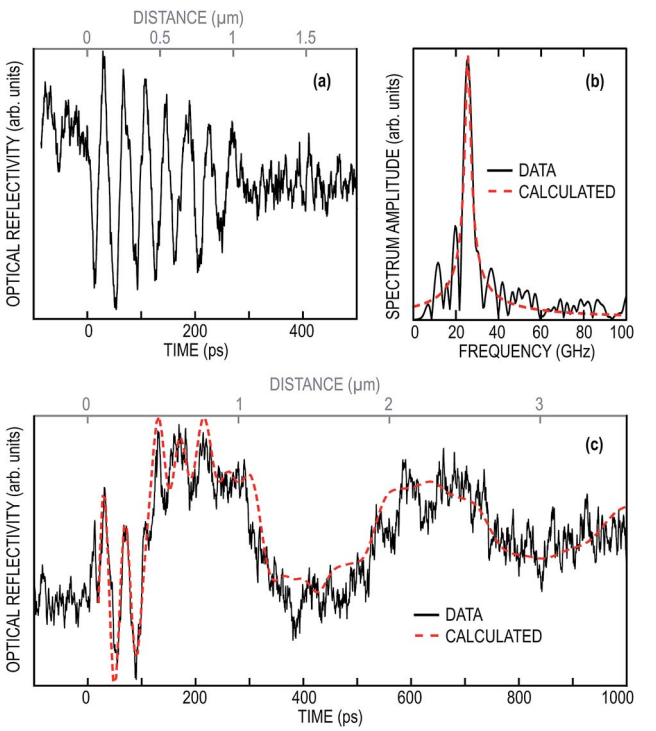

Fig. 2 (a) Optical reflectivity δR measured for the intranuclear region of a single osteosarcoma cell. (b) Measured (plain line) and calculated (dashed line, see Material and methods) amplitude of the Fourier spectrum corresponding to (a). (c) δR measured (plain line) and calculated (dashed line, see Material and methods) optical reflectivity for the intranuclear region of a single osteoblast cell.

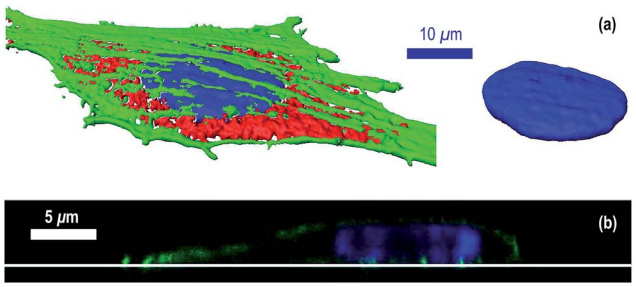

Fig. 3 (a) Confocal microscopy image of a cell with the nucleus, actin network and vinculin stained in blue, green and red, respectively (left: merge; right: nucleus). (b) Confocal microscopy image (side view) of an osteosarcoma cell with the nucleus and actin network stained in blue and green, respectively. The position of the substrate is denoted with a white horizontal line.

independently the longitudinal velocity of sound V and the nuclear thickness to match the oscillations and step-like reflectivity changes, respectively. This comparison gave a Brillouin frequency $f = 25.7$ GHz, as previously observed for this type of cells.[19] Using the measured V, the time scales in Fig. 2(a) and (c) can be converted into a distance (top gray scale). To detail the mechanics of the nucleus, we now express the rigidity of the nucleus.

2.2 Solid glass-like dynamics

To fully describe the mechanical behavior of an isotropic material, one should measure its resistance to both shearing and compression. This information is usually obtained by measuring the shear modulus G and the longitudinal modulus M, respectively. Note, however, that G and M are only rarely measured simultaneously in soft matter.[20] In the presence of viscous effects, M and G depend on the frequency. The moduli $M = M' + jM''$ and $G = G' + jG''$ are defined as complex quantities, with their real and imaginary parts describing the elastic storage and viscous losses, respectively. Here, we detect longitudinal acoustic waves, which give direct access to M.

As shown in Fig. 2(a), the compression wave is clearly underdamped ($f > \alpha$) and $M' = \rho V^2$,[21] where ρ is the mass density and $V = f\lambda/2n_r$ is the measured sound velocity. We plot in Fig. 4(a) a typical distribution of M' values obtained for single obsteoblasts, considering typical values $\rho = 1100$ kg m^{-3} and $n_r = 1.4$.[22] We obtained from this distribution $M' = 14.8 \pm 0.6$ GPa for osteoblast cells ($n = 16$) fixed with PFA (paraformaldehyde, 4%). We have also probed osteoblast cells fixed with methanol instead and obtained the same nuclear stiffness, see Fig. 4(b). This illustrates that the type of fixation has no influence on the measured stiffness at GHz frequencies.

Not surprisingly, the longitudinal modulus M' is six orders of magnitude larger than the typical values of the shear modulus G' found in the literature for cell nuclei (a few kPa at quasi-static frequencies).[6,10] Cells indeed, and to a greater extent, soft materials, are classically considered incompressible at low frequencies, with the real part of Poisson's ratio ν' approaching 0.5. At this limit, the ratio $M'/G' = 2(1 - \nu')/(1 - 2\nu')$ becomes very large.†

For comparison, we measured $M' = 2.2$ GPa in water as well as in the culture medium, 2.6 GPa in the vacuole of plant cells, and 13 GPa in the wall of plant cells,[18] using the same opto-acoustic technique at GHz frequencies. These values are summarized in Fig. 5(a). Note that the modulus of plant cell wall is 6 times larger than that of water, very close to the modulus of pure cellulose. It has been demonstrated that this high value reflects the dominant contribution of a network of cellulose fibers.[18]

Similarly, we measured a high M' value in cell nuclei. Classic Brillouin light scattering has revealed that the rigidity of proteins depends on their conformation: the M' modulus is typically ~8 GPa for DNA (as well as for most proteins),[23] and can reach ~22 GPa for dry globular proteins.[24] The high rigidity we measured, close to that of proteins in globular conformation, therefore suggests the dominant contribution of a complex

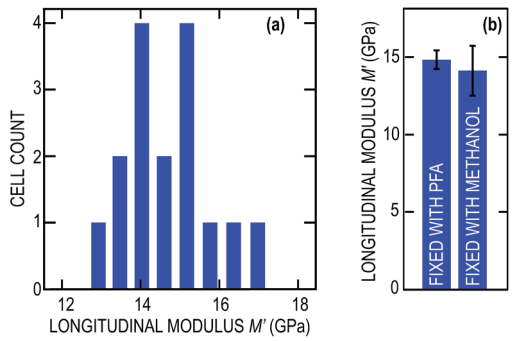

Fig. 4 (a) Typical distributions of longitudinal storage modulus M' values obtained in the intranuclear region of osteoblast cells ($n = 16$) fixed with PFA. (b) M' for the nucleus of osteoblast cells fixed with PFA ($n = 16$) or with methanol ($n = 4$).

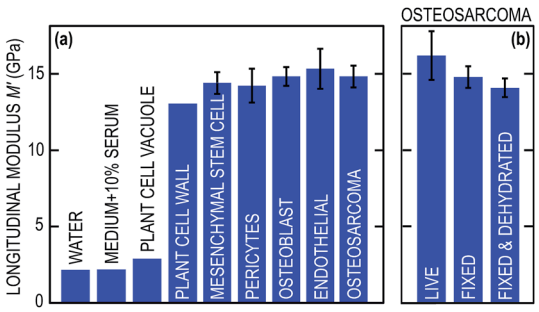

Fig. 5 (a) Longitudinal modulus M' measured for water, culture medium, vacuole of live plant cells, plant cell wall, and for the nucleus of animal cells: human mesenchymal stem cells ($n = 5$), pericyte cells ($n = 11$), osteoblast cells ($n = 16$), endothelial cells ($n = 6$) and osteosarcoma cells ($n = 4$). (b) M' for the nucleus of osteosarcoma cells in live condition, fixed with PFA, or fixed with PFA and then dehydrated with ethanol ($n = 4$). We use the Student's distribution to determine the 95% confidence interval.

† This equation is obtained considering that the imaginary part of Poisson's ratio ν'' is such that $\nu'' \ll \nu'$.

arrangement of structured proteins within the nucleus, such as chromatin fibers.

Such intricate assembly of proteins yields multiple closely spaced relaxation times. This gives rise to a glassy state that is believed to extend up to the GHz range, by analogy with polymer glasses.[6,10] In thick cells for which the lifetime $1/\alpha$ can be determined, the longitudinal loss modulus of the cell is $M'' = \rho\alpha V^2/\pi f$.[25] The typical value $\alpha = 7 \pm 3$ ns^{-1} observed with our technique at GHz frequencies in osteosarcoma cells yields $M'' = 1.3 \pm 0.5$ GPa ($n = 4$). This corresponds to a longitudinal loss tangent $\tan(\delta_L) = M''/M' \approx 0.1$, a value close to that found in glass-forming liquids[26] or soft glassy polymers[25] in the glassy state. The measured attenuation is consistent with the predicted glassy behavior of the nucleus at GHz frequencies.

The high rigidity and the low loss tangent confirm that the nucleus behaves like a solid glass in the GHz regime. Comparison with typical rigidities of proteins suggests the dominant contribution of a network of structured proteins. Let us now explore this contribution for several cell types.

2.3 Universal stiffness of the nuclear network

Building on the extrapolation far outside the kHz measurement range of magnetic bead cytometry,[10] a unique modulus has been hypothesized to exist in the cytoplasmic region at GHz frequencies. As the beads were attached to the outer surface of the cell by binding to the cytoskeleton, this behavior was attributed to a purely elastic behavior of the cytoskeletal network. Since the cytoplasm and the nucleus have similar rheological behaviors,[6] we also expect a universal stiffness of the nucleus owing to the contribution of an elastic chromatin network. To explore the GHz dynamics of such network, we probed the nuclear stiffness of vastly different cell types.

The lateral dimension of the inspected area is limited by the focusing of the laser probe beam ~3 μm, and the axial resolution of the technique is dictated by the acoustic wavelength of ~140 nm. These dimensions are smaller than the nucleus, so the probed volume consists mostly of the nucleus. It is well established however that external forces applied to the cell can be transmitted through the cytoskeleton toward the nucleus owing to the constant physical interplay between these two structures.[27] To verify that the cytoskeleton does not affect the rigidity of the nucleus we measured, we isolated nuclei, grafted them covalently to Ti6Al4V surfaces, and fixed them with PFA (see Material and methods). Fig. 6(a) and (b) show a white-light top-view and a fluorescent image (stained in DAPI) of an isolated nucleus, respectively. We plot in Fig. 6(c) the typical reflectivity measured (plain line) in isolated nuclei. Comparison with calculated waveforms yields a rigidity of ~16.4 ± 1 GPa ($n = 3$), similar to that measured for nuclei probed in entire cells. This confirms that the nucleus is the main contributor to the mechanical properties we measure in cells.

During acoustic propagation, we probe the interior of the nucleus with a ~140 nm resolution. At this scale, the interior of the nucleus can be viewed as a network of chromatin and other intranuclear components randomly oriented in a cytosol-like fluid.[8] To verify the influence of the intranuclear fluid, we

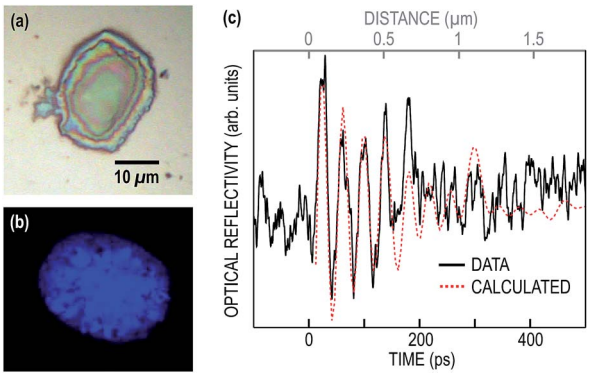

Fig. 6 (a) White-light microscopy of the isolated nucleus. Scale bar: 10 μm. (b) Fluorescent image of the isolated nucleus. (c) Typical optical reflectivity measured (plain line) and calculated (dashed line, see Material and methods) for an isolated nucleus.

probed M' for the nucleus of osteosarcoma living cells ($n = 4$), fixed with PFA (4%, $n = 4$) or fixed with PFA (4%) and then dehydrated with ethanol ($n = 4$, see Material and methods). The results are plotted in Fig. 5(c). All conditions exhibit similar M' values,‡ demonstrating that the intranuclear fluid indeed does not affect the measured stiffness. This observation confirms that the GHz compressional dynamics of the nucleus are dominated by the contribution of a solid network of chromatin fibers. We now probe this network for several cell types.

We cultured cells at various differentiation stages, ranging from stem cells to mature cells originating from greatly different tissues, including cancer cells (see Material and methods for cell culture and reagents details). We measured $M' = 14.4 \pm 0.7$ GPa ($n = 5$), 14.2 ± 1.1 GPa ($n = 11$), 14.8 ± 0.6 GPa ($n = 16$), 15.3 ± 1.3 GPa ($n = 6$), 14.8 ± 0.7 GPa ($n = 4$), for human mesenchymal stem (hMSCs), pericyte, osteoblastic, endothelial, and osteosarcoma cells, respectively. These values are summarized in Fig. 5(a). We observe a constant value of $M' \sim 15$ GPa in all mammalian cell nuclei types. This observation demonstrates the existence of a unique nuclear stiffness at GHz frequencies. Since this value is affected neither by the cytoskeleton nor by the intranuclear fluid, we attribute the unique stiffness to the contribution of an elastic chromatin network with properties that are general among all eukaryotic cells at our scale.

Our data show that the mechanical properties of the nuclei of hMSCs are similar to those of mature cells at high frequencies. This is an interesting result since hMSCs are naive cells from an epigenetic point of view, and one could have thus expected a lesser level of chromatin organization, as observed at low frequencies.[28] Extension of the universality to stem cells could be further investigated by considering different types of mesenchymal stem cells and embryonic stem cells.

‡ The two populations are identical at a 10% significance level given by a t-test. Given the sample size ($n = 4$) and the higher variance in the case of live cells, we therefore consider that the variation between the live and fixed conditions is not significant.

3 Discussion

We presented experimental data for the stiffness of single-cell nuclei in the previously unexplored GHz frequency range. We have thereby confirmed that the nucleus behaves as a solid network in this regime, and we have provided evidence that the stiffness of this network is common across various cell types. We have shown that the GHz stiffness is very close to the stiffness of highly structured proteins, such as chromatin fibers, and that it does not depend on the intranuclear fluid. These observations are consistent with the behavior of a two-phase system composed of an elastic network of chromatin fibers immersed in a cytosol-like fluid, as discussed below.

In concentrated polymers solutions, the large number of strong mechanical contacts between the polymer chains limit their motion. For this, concentrated polymer solutions are usually described as an elastic network invaded by the solvent.[29] The acoustic wavelength in our experiment, $\lambda/2n_r \sim 140$ nm, is larger than the average distance between the entanglements, so homogenization theories apply. Classical approaches to sound propagation in such systems[29] predict the existence (in addition to shear modes which are not considered here) of a slow diffusive longitudinal mode and a fast propagative longitudinal mode, corresponding to the motion of the fluid and of the network, respectively. In the presence of friction forces between the viscous fluid and the network, $\boldsymbol{F} = -2\rho\boldsymbol{\nu}/\tau$ (where $\boldsymbol{\nu}$ is the velocity of the network relative to the fluid), these two modes are coupled, resulting in attenuation of the modes with a relaxation time τ.

However, we measured an underdamped propagative mode that is not influenced by the presence of the intranuclear fluid, suggesting that the frequency of the acoustic wave ω is larger than $1/\tau$. In this case, the velocity and attenuation of the fast mode we measure are that of the network and are not influenced by friction. One view of this is that friction locks the fluid onto the network at high frequencies: they therefore undergo the same deformation and behave as an isostrain system. The effective modulus of this two-phase system, M_e, can thus be merely obtained by a Voigt average of the moduli of the network and of the fluid, M_n and M_f, respectively, weighted by their respective volume fractions, ϕ and $1-\phi$: $M_e = \phi M_n + (1-\phi)M_f$. Considering that the network is much stiffer than the fluid, $M_f \ll M_n$, the effective modulus is close to that of the network itself, $M_e \approx \phi M_n$. For illustration, typical values $M_n = 22$ GPa (close to a protein in globular conformation[24]) and $\phi = 0.7$§ give $M_e = 15.4$ GPa, a value close to our measurement, demonstrating that we indeed probed the modulus of the network.

We now discuss the origin of sound attenuation at GHz frequencies in this network-based system. We have obtained a longitudinal loss tangent $\tan\delta \sim 0.1$, suggesting that the glassy behavior of the nucleus extends up to GHz frequencies, as generally believed by analogy with polymer glasses.[6,10] Since $\omega \gg 1/\tau$, this metastable behavior is dictated by the multiplicity of internal degrees of freedom of the network itself at GHz frequencies, rather than by the fluid or friction at the fluid–network interface. As the frequency decreases ($\omega \sim 1/\tau$), friction forces should decrease and fluid–network relative motion should contribute increasingly to mechanical relaxation within the nucleus. Measurements at intermediate frequencies, filling the gap between the ranges accessible by microrheology and by light scattering techniques, should allow determining the balance between friction and metastable motion of the network, thus providing a deeper understanding of the relation between the glassy state and the microstructure of the nucleus. These results complement our knowledge of the mechanical properties of the nucleus and open the way to the investigation of network-dynamics of the nucleus during various biological processes, such as differentiation, replication or morphogenesis.

§ Such concentration is half-way between concentrated polymer solution and polymer melts. For comparison, the volume fraction of hemicelluloses in the wall of plant cells is 0.7 (ref. 18).

4 Material and methods

4.1 Opto-acoustic setup

Optical pump pulses with a duration of 100 fs emitted by a Ti:sapphire mode-locked laser are initially absorbed in Ti6Al4V over a distance comparable to the optical skin depth, approximately 15 nm,[30] in the vicinity of the Ti6Al4V-cell interface. The ensuing ultrafast thermal dilatation launches a longitudinal coherent-phonon pulse, with a broad spectrum extending up to ~200 GHz. The pump light is modulated at 330 kHz by an acousto-optic modulator to provide reference frequency and phase for lock-in detection. The reflectivity change δR is measured with probe pulses as a function of the pump-probe time delay, provided by the displacement of a mechanical delay line. The probe is frequency-doubled by a non-linear Beta Barium Borate (BBO) crystal. The low-energy coaxial pump (wavelength 800 nm, energy 3 pJ) and frequency-doubled probe ($\lambda = 400$ nm, 1.5 pJ) beams are focused through the top of the nuclear region at the Ti6Al4V-cell interface by a ×20 objective lens (Nikon, NA 0.45) to spots of radii ~5 and ~3 μm (at $1/e^2$), respectively.

4.2 Photoacoustic modelling

We model the photoelastic interaction as detailed in ref. 31. We first describe the acoustic generation. The radius of the Gaussian probe beam is by one order of magnitude larger than the wavelength of the acoustic phonons and no acoustic diffraction occurs. The cell is thus described as a finite layer lying on a semi-infinite Ti6Al4V half-space. The temperature rise $T_t(x, t)$ in Ti following laser absorption in Ti6Al4V is described by the Fourier equation, using the thermal properties of pure Ti.[30] The propagation of the longitudinal strain $\eta_c(x, t)$ in the cell resulting from the thermal dilatation $\alpha_t \Delta T_t$ of Ti, where α_t is the rigidity-dilatation constant of Ti, is described by a one-dimensional wave equation. A damping of the form $\exp(-\Gamma x)$ accounts for phonon attenuation Γ in the cell.

The detection mechanism is modelled as follows. Qualitatively speaking, part of the probe beam is back-scattered by the strain wave that propagates within the cell at velocity V and

interferes with the static part of the beam that is reflected at the Ti surface. These interferences give rise to oscillations of the optical reflectivity δR at a frequency $f = 2V/\lambda_c$, where λ_c is the laser probe wavelength in the cell. In addition, when the acoustic wave impinges on the free surface of the cell, there is a sudden change in the cell thickness.[32,33] This induces a step-like variation of the optical reflectivity at times $\sim(2m-1)d/V$, where d is the cell thickness and m is an integer counting the m^{th} acoustic reflection.

For a more quantitative calculation of this photoelastic interaction, we write that the strain $\eta_c(x, t)$ modulates the dielectric permittivity of the cell of a quantity $\delta\varepsilon(x, t) \propto \eta(x, t)$. The optical reflectivity change δR is obtained by solving Maxwell's equation written for dielectric permittivity $\delta\varepsilon(x, t)$ modulated by sound propagation.[15] This model allows determining simultaneously and independently the sound velocity of the cell V and its thickness d.

4.3 Cell culture and reagents

We studied cells originating from vastly different tissues, healthy or diseased: bone marrow mesenchymal stem cells, pericytes from the perivascular region, osteoblasts from the bone extracellular matrix, vascular endothelial cells, as well as cancer cells. We cultured cells on a Ti6Al4V metal alloy, a typical biomaterial used for bone implants,[34] to ensure photoelastic transduction and to prevent corrosion and ion release. Fig. 1(a) shows a typical white-light image of an osteoblast cell.

Primary human (bone marrow) mesenchymal stem cells (Lonza, Switzerland) were cultured in a minimum essential medium (Alpha-MEM, Gibco) supplemented with 10% (vol/vol) fetal bovine serum (FBS), 1% penicillin/streptomycin and incubated in a humidified atmosphere containing 5% (vol/vol) CO_2 at 37 °C. Human osteosarcoma cells (MG63; ATCC, France) and human endothelial cells (HUVECs; Promocell, France) were cultured in IMDM medium (Invitrogen) supplemented with 10%FBS (Invitrogen) and 1% penicillin/streptomycin (Invitrogen). Human pericytes (Promocell, France) were maintained in a pericyte growth medium (Promocell, France). A mouse progenitor osteoblast cell line (MC3T3-E1; ATCC, France) was cultured in alpha-MEM (GIBCO) supplemented with 10% FBS and 1% penicillin/streptomycin. All cells were used at low passage numbers (passage 4 to 8), subconfluently cultured and plated at 10^4 cells per cm^2.

Concerning the dehydrated cell condition, the cells were first washed with 1X PBS and were then fixed with paraformaldehyde (4%) diluted in PBS for 20 min at 4 °C. The samples were finally dehydrated in increasing concentrations of ethanol (30, 70, 80, 90, 95 and 100%). Concerning the fixation of cells with methanol, cultured cells were first washed with 1× PBS and were put with methanol (80%) at −20 °C for 15 min.

4.4 Isolation of cell nuclei and covalent grafting on titanium surfaces

Nuclei were isolated with a Nuclei Isolation Kit (Nuclei EZ Prep, Sigma).[35,36] Cells were harvested by scraping in phosphate-buffered saline (PBS 1×) or by trypsinization and collected by centrifugation before being lysed in detergent-containing lysis buffer. Contamination by endogenous proteases or nucleases and extraction or physical perturbations by detergents may have adverse effects on the quality of the nuclei. The nuclei may become more fragile due to the loss of nuclear membranes, and consequently, the purified nuclei may aggregate if excessive DNA leakage occurs. In our experiments, these potential problems were overcome by rapidly isolating the nuclei from fresh cells and by keeping the nuclei cold (4 °C) during the isolation procedure.

Note that we have measured the mechanical properties of the interior of these isolated nuclei without contact using acoustic waves. Techniques that rely on direct mechanical contact to the nucleus to assess the mechanical properties (AFM, micropipette) may be more sensitive to alteration of the nuclear membrane. For such studies that focus on the envelope or lamina structure, extra care should be taken to preserve the mechanical integrity of the nuclear envelope.[7]

The nuclei were then covalently grafted to Ti–6Al–4V surfaces, similarly to peptides, proteins or nanoparticles.[37,38] The strategy of nuclei immobilization involves (i) grafting of an amino-functional organosilane (APTES, three-aminopropyltriethoxysilane) onto the surface of Ti6Al4V, (ii) substitution of the terminal amine for a hetero-bifunctional cross-linker (SMP, 3-succinimidyl-3-maleimidopropionate) to (iii) react the outer maleimide group with a protein in the membrane due to the presence of a thiol group in the terminal cysteine. The nuclei were incubated for 10 to 15 min with active Ti–6Al–4V surfaces and then fixed with paraformaldehyde (PFA 4%) in PBS (4 °C) for 15 min.

4.5 Cell staining

After 12 hours of culture, the cells on the surfaces were fixed for 30 min in 4% paraformaldehyde/PBS at 4 °C. After fixation, the cells were permeabilized in 1% Triton X-100 in PBS for 15 min. Actin and vinculin were visualized by treating the cells with 1% (v/v) phalloidin-FITC (Sigma) and mouse monoclonal anti-vinculin (Invitrogen) for 1 hour at 37 °C. The cells were then incubated with an Alexa Fluor 588-conjugated $F(ab')_2$ fragment of rabbit anti-mouse IgG(H + L) for 30 minutes at room temperature. The cell nuclei were counterstained in 20 ng mL^{-1} DAPI for 10 min at room temperature. The confocal images were produced using a Leica SP5 confocal microscope and MetaMorph software.

Acknowledgements

We thank C. Chanseau, J. Kalisky and V. Gocheva. This work was supported by the Region Aquitaine, the GIS Advanced Materials in Aquitaine and the Agence Nationale pour la Recherche (Grant No. ANR-13-BS09-0021-01).

References

1 P. Isermann and J. Lammerding, *Curr. Biol.*, 2013, **23**, R1113–R1121.

2 Y. Sunada, S. M. Bernier, A. Utani, Y. Yamada and K. P. Campbell, *Hum. Mol. Genet.*, 1995, **4**, 1055–1061.
3 T. Sullivan, D. Escalante-Alcalde, H. Bhatt, M. Anver, N. Bhat, K. Nagashima, C. L. Stewart and B. Burke, *J. Cell Biol.*, 1999, **147**, 913–920.
4 J. D. Pajerowski, K. N. Dahl, F. L. Zhong, P. J. Sammak and D. E. Discher, *Proc. Natl. Acad. Sci. U. S. A.*, 2007, **104**, 15619–15624.
5 M. L. Lombardi and J. Lammerding, *Nuclear Mechanics & Genome Regulation*, Academic Press, 2010, vol. 98, pp. 121–141.
6 Y. Tseng, J. S. H. Lee, T. P. Kole, I. Jiang and D. Wirtz, *J. Cell Sci.*, 2004, **117**, 2159–2167.
7 K. N. Dahl, A. J. Engler, J. D. Pajerowski and D. E. Discher, *Biophys. J.*, 2005, **89**, 2855–2864.
8 M. Wachsmuth, W. Waldeck and J. Langowski, *J. Mol. Biol.*, 2000, **298**, 677–689.
9 E. Moeendarbary, L. Valon, M. Fritzsche, A. R. Harris, D. A. Moulding, A. J. Thrasher, E. Stride, L. Mahadevan and G. T. Charras, *Nat. Mater.*, 2013, **12**, 253–261.
10 B. Fabry, G. N. Maksym, J. P. Butler, M. Glogauer, D. Navajas and J. J. Fredberg, *Phys. Rev. Lett.*, 2001, **87**, 148102.
11 D. Stamenovic, *Nat. Mater.*, 2006, **5**, 597–598.
12 G. Scarcelli and S. H. Yun, *Nat. Photonics*, 2008, **2**, 39–43.
13 J. Rheinlaender and T. E. Schaffer, *Soft Matter*, 2013, **9**, 3230–3236.
14 L. M. Rebelo, J. S. de Sousa, J. M. Filho and M. Radmacher, *Nanotechnology*, 2013, **24**, 055102.
15 C. Thomsen, H. T. Grahn, H. J. Maris and J. Tauc, *Phys. Rev. B: Condens. Matter Mater. Phys.*, 1986, **34**, 4129–4138.
16 H. J. Maris, *Sci. Am.*, 1998, **278**, 64–67.
17 A. Simon and M.-C. Durrieu, *Micron*, 2006, **37**, 1–13.
18 A. Gadalla, T. Dehoux and B. Audoin, *Planta*, 2014, **239**, 1129–1137.
19 M. Ducousso, O. El-Farouk Zouani, C. Chanseau, C. Chollet, C. Rossignol, B. Audoin and M.-C. Durrieu, *Eur. Phys. J.: Appl. Phys.*, 2013, **61**, 11201.
20 C. Verdier, P.-Y. Longin and M. Piau, *Rheol. Acta*, 1998, **37**, 234–244.
21 T. A. Litovitz and C. M. Davis, in *Physical Acoustics*, ed. W. P. Mason, Academic, New York, 1965, vol. 2A.
22 A. Brunsting and P. F. Mullaney, *Biophys. J.*, 1974, **14**, 439–453.
23 S. A. Lee, S. M. Lindsay, J. W. Powell, T. Weidlich, N. J. Tao, G. D. Lewen and A. Rupprecht, *Biopolymers*, 1987, **26**, 1637–1665.
24 S. Speziale, F. Jiang, C. Caylor, S. Kriminski, C.-S. Zha, R. Thorne and T. Duffy, *Biophys. J.*, 2003, **85**, 3202–3213.
25 T. Dehoux, N. Tsapis and B. Audoin, *Soft Matter*, 2012, **8**, 2586–2589.
26 T. Pezeril, C. Klieber, S. Andrieu and K. A. Nelson, *Phys. Rev. Lett.*, 2009, **102**, 107402.
27 N. Wang, J. D. Tytell and D. E. Ingber, *Nat. Rev. Mol. Cell Biol.*, 2009, **10**, 75–82.
28 A. J. Ribeiro, S. Tottey, R. W. Taylor, R. Bise, T. Kanade, S. F. Badylak and K. N. Dahl, *J. Biomech.*, 2012, **45**, 1280–1287.
29 T. Tanaka, L. O. Hocker and G. B. Benedek, *J. Chem. Phys.*, 1973, **59**, 5151–5159.
30 B. Audoin, C. Rossignol, N. Chigarev, M. Ducousso, G. Forget, F. Guillemot and M. C. Durrieu, *Ultrasonics*, 2010, **50**, 202–207.
31 M. Ducousso, T. Dehoux, B. Audoin, O. Zouani, C. Chollet and M. C. Durrieu, *J. Phys.: Conf. Ser.*, 2011, **269**, 012024.
32 C. Rossignol, B. Perrin, S. Laborde, L. Vandenbulcke, M. De Barros and P. Djemia, *J. Appl. Phys.*, 2004, **95**, 4157–4162.
33 O. B. Wright, *J. Appl. Phys.*, 1992, **71**, 1617–1629.
34 I. Tognarini, S. Sorace, R. Zonefrati, G. Galli, A. Gozzini, S. C. Sala, G. D. Z. Thyrion, A. M. Carossino, A. Tanini, C. Mavilia, C. Azzari, F. Sbaiz, A. Facchini, R. Capanna and M. L. Brandi, *Biomaterials*, 2008, **29**, 809–824.
35 P. Juin, M. Pelletier, L. Oliver, K. Tremblais, M. Grégoire, K. Meflah and F. M. Vallette, *J. Biol. Chem.*, 1998, **273**, 17559–17564.
36 Y. A. Lazebnik, S. Cole, C. A. Cooke, W. G. Nelson and W. C. Earnshaw, *J. Cell Biol.*, 1993, **123**, 7–22.
37 M. C. Porté-Durrieu, F. Guillemot, S. Pallu, C. Labrugère, B. Brouillaud, R. Bareille, J. Amédée, N. Barthe, M. Dard and C. Baquey, *Biomaterials*, 2004, **25**, 4837–4846.
38 L. Pichavant, C. Bourget, M.-C. Durrieu and V. Héroguez, *Macromolecules*, 2011, **44**, 7879–7887.